Electrochimica Acta 338 (2020) 135902

Contents lists available at ScienceDirect

Electrochimica Acta

journal homepage: www.elsevier.com/locate/electacta

Anion-inhibited solid framework polymer electrolyte for dendrite-free lithium metal batteries

Wenyan Shang [1], Chaoqun Niu [1], Guangping Chen , Yubing Chen , Jie Du *

State Key Laboratory of Marine Resource Utilization in South China Sea, College of Materials Science and Engineering, Hainan University, Haikou, 570228, China

ARTICLE INFO

Article history:
Received 21 December 2019
Received in revised form
12 February 2020
Accepted 12 February 2020
Available online 14 February 2020

Keywords:
Lithium metal battery
Anion inhibition
Solid framework structure
Dendrite-free

ABSTRACT

Lithium metal shows great promise as an anode material for high-performance next-generation batteries due to its low redox potential, low weight, and high specific capacity. However, the uncontrolled growth of lithium dendrites during charge–discharge cycling limits the practical application of lithium metal anodes. In this work, an anion-inhibited solid framework polymer electrolyte (SFPE) was prepared through the polymerization of vinyl polyhedral oligomeric silsesquioxane (VPOSS) and diallyl dicarbonate (DDC) as a means to suppress lithium dendrite formation. The structure of the electrolyte was found to reduce the electric field at the anode surface by restricting the free movement of the anions ($TFSI^-$) of the lithium salt, which facilitated the orderly, uniform, and safe deposition of lithium ions on the anode. The SFPE presented a high lithium ion transference number (0.63), a wide window of electrochemical stability (5.6 V versus Li^+/Li), and high ionic conductivity (0.31 mS cm^{-1}) at 25 °C. A $LiFePO_4$/Li cell containing the SFPE achieved a specific discharge capacity of 165 mAh g^{-1} and a capacity retention of 91.3% after 200 cycles at 0.1 C (1 C = 180 mAh g^{-1}) and 25 °C, and the lithium anode surface remained smooth after 600 h of constant-current charge–discharge cycling. Based on these results, this SFPE is an excellent candidate for use in high-performance lithium metal batteries.

1. Introduction

Due to their limited energy capacities, traditional lithium-ion batteries (LIBs) cannot meet the increasing demand for high energy density of batteries that can be used in modern electronics [1]. Lithium metal has attracted great interest as a potential anode material for next-generation recyclable batteries due to its high specific capacity (3860 mAh g^{-1}), lowest redox potential (−3.04 V vs. the standard hydrogen electrode H^+/H_2), and lowest weight (0.53 g cm^{-3}) [2]. However, the nonuniform deposition of lithium ion on the Li metal anode surface during charge–discharge cycling leads to the uncontrolled growth of lithium dendrites [3], which seriously impedes the practical application of lithium metal batteries. More importantly, lithium dendrites can pierce the separator, increasing the risk of a short circuit and thermal runaway, which could lead to burning or explosion [4]. Considerable research effort has been directed into methods of overcoming this problem through the use of, for example, additives or advanced separators [5,6]. Unfortunately, the reaction between the existing liquid electrolytes and highly reactive lithium metal is the root of the potential safety hazard [7]. Therefore, replacing liquid electrolytes with solid polymer electrolytes (SPEs) is a smart choice [5,8]. Among SPEs, polycarbonate-based SPEs have high lithium ion conductivities due the presence of the carbonate group. However, lithium dendrite growth restricts the cycling performance of solid polymer electrolytes [9]. Therefore, a polycarbonate-based SPE material capable of inhibiting lithium dendrite formation and thus reducing the growth of Li dendrites induced by strong space charge near the anode is urgently required [10–12].

One candidate for such material is vinyl polyhedral oligomeric silsesquioxane (VPOSS), which consists of an inorganic skeleton and organic components [13]. The inorganic cage structure of VPOSS can play a role of modified like other inorganic filler [14], improving the thermal stability and reducing the crystallinity of the polymer, while the organic components form an organic phase on the inorganic cage surface that reduces the surface energy to prevent agglomeration [15]. Indeed, in theory, the application of an ordered solid framework structure based on a combination of

* Corresponding author.
E-mail address: dujie@hainanu.edu.cn (J. Du).
[1] Authors contributed equally.

https://doi.org/10.1016/j.electacta.2020.135902
0013-4686/

VPOSS and polymerized diallyl dicarbonate (PDDC) should cause the anions ($TFSI^-$) in lithium metal batteries to become fixed in the solid polymer electrolyte, leading to a homogeneous distribution of space charge and lithium ions, thus facilitating dendrite-free lithium deposition.

In this work, an anion-inhibited solid framework polymer electrolyte (SFPE) with a wide electrochemical stability window up to 5.6 V, a high lithium-ion transference number (i.e., fraction of the total charge conducted in the electrolyte that is transferred by lithium ions) of 0.63, and high ionic conductivity of 0.31 mS cm^{-1} was prepared. LFP/SFPE/Li cells incorporating this electrolyte were found to exhibit a discharge capacity retention rate of 91.3% after 200 charge–discharge cycles at 0.1 C (1 C = 180 mAh g^{-1}) and 25 °C. Also, lithium dendrites were not observed on the lithium anode surface after 600 h of constant-current charge–discharge cycling of the Li/SFPE/Li cells. This SFPE synthesized by in-situ polymerization is therefore a promising candidate for use in safe next-generation LMBs with high performance.

2. Experimental section

2.1. Materials

The materials used in this study were as follows: $LiFePO_4$ (Canrd, 98%); ketjenblack carbon black (KB, AkzoNobel N.V., battery grade); polyvinylidene fluoride (PVDF, Solvay, battery grade); bistrifluoromethanesulfonimidate (LiTFSI, Aladdin, 99.0%); N-methyl-2-pyrrolidone (NMP, Aladdin, GC); diallyl dicarbonate (DDC, TCI, > 95.0%); vinyl polyhedral oligomeric silsesquioxane (VPOSS, Macklin, 98%); and azodiisobutyronitrile (AIBN, Aladdin, 99.0%). All reagents were purchased commercially and stored in an argon glove box.

2.2. Preparation of $LiFePO_4$ cathode

The $LiFePO_4$ (LFP) cathode sheet was obtained by uniformly coating the composite onto Al foil and then vacuum drying at 110 °C for 12 h. The composite comprised $LiFePO_4$ powder, KB, PVDF (wt%, 8:1:1) and was fully ground. Finally, a LFP cathode with an active substance load of about 2.5 mg cm^{-2} was obtained.

2.3. Preparation of SFPE

To prepare the SFPE, LiTFSI (1 M), AIBN (1 wt%), and VPOSS (1 wt %) were dissolved in diallyl dicarbonate (DDC) and stirred for 6 h at 25 °C to form a uniform precursor solution. When the battery was assembled, 40-μl precursor droplets were applied as electrolyte to both sides of the separator, and SFPE cells were obtained by fully polymerizing the electrolyte at 60 °C for 24 h. All of the above operations were carried out in the argon glove box (water content $\leq$ 1 ppm).

2.4. Structure characterization

Structural characterization was performed using several techniques. Differential scanning calorimetry was realized using a DSC Q2000 differential calorimeter (TA Instruments) in the range 60–600 °C at a heating rate of 10 °C min^{-1} under a nitrogen atmosphere. Five-milligram samples were used. The mechanical properties of the PDDC and SFPE were evaluated using a WDW-1 universal tension–compression testing machine operating at a speed of 1 mm min^{-1}. Sample morphology was examined using scanning electron microscopy (SEM), employing a Phenom Prox instrument. Samples were also investigated with attenuated total reflection Fourier transform infrared spectroscopy (ATR-FTIR) in the range of 4000–400 cm^{-1}.

2.5. Electrochemical testing

The ionic conductivity (σ) of the PDDC and SFPE was tested in SS/PDDC-SPE/SS and SS/SFPE/SS (SS: stainless steel) coin cells at various temperatures (25–70 °C) using AC impedance spectroscopy over the frequency range from 10^{-1} to 2×10^6 Hz and at a rate of 10 mV. The electrochemical stability window of the SFPE was evaluated using a Li/SFPE/SS coin cell by performing cyclic voltammetry (CV) in the voltage range of 0–7 V at a scanning rate of 0.1 mV s^{-1} and 25 °C. Symmetric Li/SFPE/Li cells were applied to test the Li-ion transference number (t_+) of the SFPE at 25 °C and to measure the polarization by charging and discharging at constant current. The electrochemical stability was characterized using LFP/SFPE/Li coin cells and a LAND CT 2001A battery test system over the potential range 2.5–4.0 V at 25 °C. All cells were assembled in an argon-filled glove box.

3. Results and discussion

During charge–discharge cycling, a low lithium-ion transference number exacerbates nonuniform lithium deposition, leading to the continuous production of lithium dendrites [16,17]. As shown in Fig. 1, we prepared an anion-inhibited SPE to protect the Li anode by constructing an electrolyte with a solid framework structure.

The specific steps performed to achieve SFPE are shown in Fig. S1. During this process, DDC and VPOSS were copolymerized to form an ordered frame structure with polymer chains that become mechanically entangled with $TFSI^-$ anions. After polymerization, these anions become fixed in the ordered solid framework structure since the SFPE interacts with the anions ($TFSI^-$ acts as a Lewis acid with a shared pair of electrons) [18]. According to space-charge theory, the presence of space charge near the anode can induce an uneven distribution of lithium ions in this region, encouraging nonuniform Li deposition. Suppressing the free movement of anions leads to a harmonious environment that inhibits the formation of space charge near the anode, which in turn promotes uniform Li deposition.

3.1. Characterization of SFPE

The morphology of the SFPE was examined in detail using SEM. As shown in Fig. 2a, the SFPE exhibits a distinct ordered framework structure that provides the basis for anion inhibition.

The FTIR-ATR spectra are shown in Fig. 2b. In order to better study the nature of the polymerization reaction, we conducted a comparative analysis of the spectra of DDC, VPOSS, LiTFSI and SFPE.

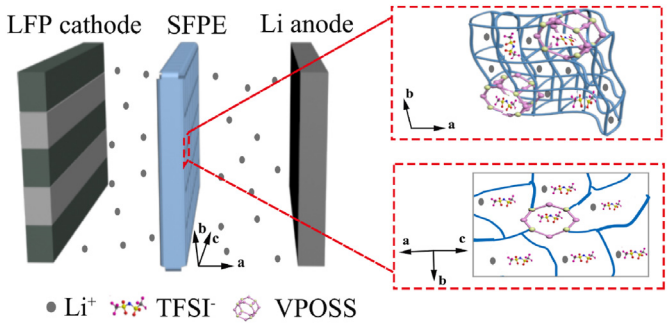

Fig. 1. Schematic of the SFPE in a lithium metal battery, showing anions immobilized in the framework of the SFPE.

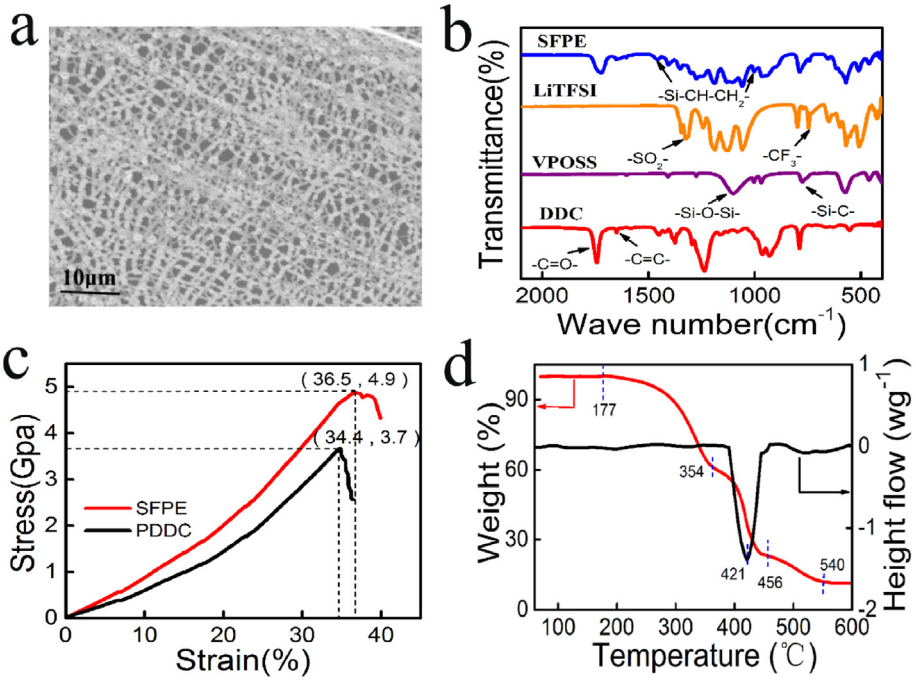

Fig. 2. Physical and chemical properties of PDDC and the SFPE: (a) SEM image of a cross-section of the SFPE; (b) FT-IR spectra of DDC, VPOSS, LiTFSI, and the SFPE; (c) stress and strain curves for PDDC and the SFPE; (d) DSC-TGA curve for the SFPE polymerized in situ.

The disappearance of the peak at 1646 cm^{-1} from C═C bonds [19] after polymerization indicates that the polymerization is complete. The peak at 1746 cm^{-1} derives from vibrations of the −C═O group in DDC, while the peak at 1100 cm^{-1} is related with stretching vibrations of -Si-O-Si- in VPOSS cages. The well-defined peak at 771 cm^{-1} relates to the -Si−C- group, whereas the sharp peaks at 1457 cm^{-1} and 992 cm^{-1} result from -Si-CH═CH_2- bending vibrations in VPOSS. The peak at 1318 cm^{-1} for LiTFSI is from antisymmetric stretching of the −SO_2- group. The fact that this peak is weaker and narrower in the spectrum of SFPE illustrates that LiTFSI interacts strongly with DDC in the system. This is why the lithium-ion transference number of SFPE is relatively high (0.63), as discussed later. The peaks at 1248 and 748 cm^{-1} represent the symmetric tensile vibrations and deformation vibrations of the −CF_3- group. The stability of those peaks illustrate that LiTFSI is stable in SFPE, which is the basis for stable battery cycling [20]. The stress−strain curve shown in Fig. 2c, the SFPE can withstand a maximum stress of 4.88 GPa when the deformation is 36.7% and has a higher compressive strength than PDDC alone, which suggests that the use of SFPE rwather than PDDC alone should enhance battery safety during transportation and when the battery is subjected to external forces. Thermal stability is an important influence on battery safety performance. Conventional liquid electrolytes show poor stability at high temperatures and are prone to combustion and explosion. The DSC-TGA curves of SFPE and PDDC are shown in Fig. 2b and S2, respectively. The severe weight loss observed for PDDC and SFPE above 177 °C indicates that they both start to decompose rapidly at this temperature. The weight loss of carbon in the polymer shows a drop in block velocity at 388 °C for PDDC and 404 °C for SFPE. Finally, the curves for PDDC and SFPE reach a steady state at 472 and 540 °C, respectively. High thermal stability also lays the foundations for battery cycle stability at different temperatures.

Other influences on the cycling performance of a battery include the molecular weight of the polymer. As shown in Fig. S2, the molecular weight of the SFPE can reach 6.8 × 10^4. High molecular weight determines that SFPE has sufficient long segments for continuous lithium ion conduction.

3.2. Electrochemical performance of SFPE

The ionic conductivity of lithium metal batteries has a significant impact on its practical applications. Fig. 3a shows Nyquist plots obtained over the frequency range from 0.1 to 2 × 10^6 Hz at a rate of 10 mV for SS/PDDC-SPE/SS and SS/SFPE/SS coin cells. The semicircle observed at high frequency was used to calculate the ionic conductivity based on the thickness of the prepared electrolyte film and the area of the electrode. The straight line at low frequency relates to the migration of lithium ions and is indicative of the uneven nature of the interface. Due to the introduction of inorganic components, the impedance of the SFPE (153 Ohm) was found to be larger than that of the PDDC-SPE (129 Ohm). The calculated ionic conductivity of SFPE was 0.31 mS cm^{-1} at 25 °C. The impedance of SFPE and that of PDDC at various temperatures are shown in Figs. S4 (a) and S5(a), respectively. The impedance was observed to decrease with increasing temperature, which is caused by increased flow of polymer segments at high temperatures. The relationship between temperature and the ionic conductivity is shown in Fig. S4 (b) for the SFPE and in Fig. S5(b) for PDDC. According to the Arrhenius equation, the activation energy (Ea) for lithium ion conduction is 0.20 eV in SFPE and 0.15 eV in PDDC. LFP/SFPE/Li coin cells were also assembled and tested for impedance over the frequency range from 10^{-1} to 2 × 10^6 Hz at a rate of 10 mV after 200 cycles, the results are shown in Fig. S6 (a).

As depicted in Fig. 3b, CV curves were also obtained for the Li/PDDC-SPE/SS and Li/SFPE/SS cells at a scan rate of 0.1 mV s^{-1} and 25 °C. The SFPE exhibited a stable voltage window up to 5.6 V, slightly higher than that for the PDDC SPE (5.4V). Li/SFPE/LFP coin cells were assembled and their cycle stability was tested. No significant oxidation or reduction peak was observed in the voltage range from 2.0 to 4.5 V (see Fig. S6 (b)).

The lithium-ion transference number (t_+) is a decisive factor

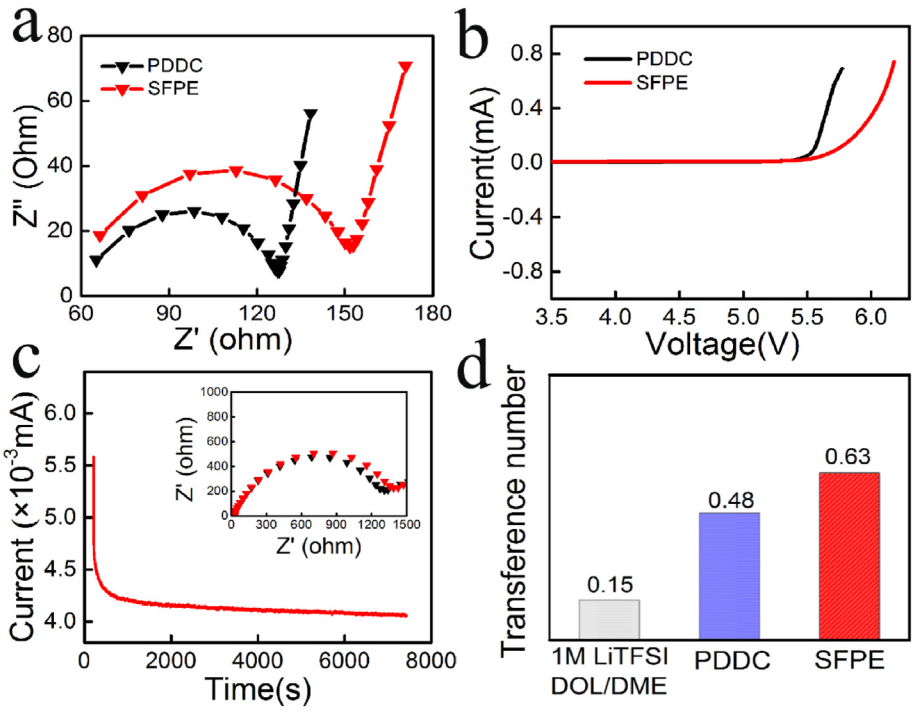

Fig. 3. Comparison of the electrochemical performance of PDDC and the SFPE: (a) Nyquist plots of the impedance spectra of SS//SS cells; (b) cyclic voltammetry curves of Li//SS cells; (c) variation of the current with time during the polarization of the symmetric Li/SFPE/Li cell under an applied polarization potential of 10 mV (the inset graph shows the impedance before and after polarization at 25 °C); (d) lithium-ion transference numbers for a liquid electrolyte, PDDC, and the SFPE.

affecting the ability of lithium ions to transfer charge and the rate performance of lithium batteries. t_+ was determined by observing the variation in the current over time during the polarization of Li/SFPE/Li cells under a polarization voltage of 10 mV (see Fig. 3c) and then applying the following equation:

$$t_+ = \frac{I_S(\Delta V - I_0 R_0)}{I_0(\Delta V - I_S R_S)}$$

The t_+ value of the SFPE was calculated to be 0.63. Fig. 3d compares the t_+ values of a liquid electrolyte (0.15), PDDC (0.47; Variation of the current with time during the polarization is shown in Fig. S7), and the SFPE. The enhanced t_+ value of the SFPE indicates that the solid frame structure of SFPE effectively inhibits the movement of anions and provides better protecting of the Li metal anode from the effects of anion movement.

3.3. The formation and morphology of lithium dendrites

By simulating the distribution of lithium ions on the lithium metal anode surface, the advantage of solid framework structure SFPE is illustrated. As shown in Fig. 4a, when an electric field is applied to a liquid electrolyte containing free anions, the anions will tend to interact with cations moving in the opposite direction, leading to the gradual formation of a barrier to cation migration [21]. This causes a steep concentration gradient of lithium ions from the bulk electrolyte to the anode surface, and this nonuniform distribution of lithium ions leads to the undesirable generation of lithium dendrites [22]. Lithium dendrite growth is partially inhibited through the use of a polycarbonate electrolyte such as PDDC (Fig. 4b) because the carbonate groups of the electrolyte can coordinate with lithium ions, creating fast lithium-ion transport channels [23]. The utilization of an electrolyte with a solid framework structure (Fig. 4c) suppresses the formation of space charge by inhibiting the free movement of anions, which, in turn, promotes the uniform distribution of lithium ions and the formation of a dendrite-free lithium anode. SEM images of the lithium metal surfaces in various Li//Li cells after 600 h of constant-current charge–discharge cycling are shown in Fig. 4d–f. After cycling, the lithium metal surfaces of the Li/liquid electrolyte/Li (Fig. 4d) and Li/PDDC-SPE/Li (Fig. 4e) cells show significant (albeit different degrees of) lithium dendrite formation due to uneven deposition behavior of the lithium at the electrolyte interface during lithium ion plating and stripping. Conversely, the lithium metal surface in the Li/SFPE/Li cell (Fig. 4f) remains smooth after cycling.

3.4. The cycle performance of Li//LFP

The cycle stabilities of the Li/PDDC-SPE/Li and Li/SFPE/Li cells were compared by performing galvanostatic cycling tests, which involved implementing repeated charge–discharge cycles for 600 h at 0.1 mA cm^{-2} and 25 °C. As shown in Fig. 5a, the voltage of the Li/PDDC-SPE/Li cell start to increase after remaining stable for 80 h, and the battery is shorted after 226 h. This indicates that polarization of the lithium metal battery increased and lithium dendrites gradually formed and enlarged on the surface of lithium anode during cycling. In contrast, the voltage for Li plating/stripping in the Li/SFPE/Li cell remained steady even after 600 h, indicating that the SFPE effectively inhibits Li dendrite formation.

In order to further examine the influence of the SFPE in lithium-based batteries, symmetric lithium batteries were assembled in an argon-filled glove box and cycled at various current densities and 25 °C. As Fig. 5b shown, the cell overpotential was found to be only around 10 mV at 0.025 mA cm^{-2} and around 50 mV at 0.1 mA cm^{-2}, which is consistent with the overpotentials of symmetric lithium-based cells containing the most advanced polymer electrolytes [24]. When the current density was increased to 0.2 mA cm^{-2}, the overpotential of the symmetrical battery increased to 100 mV due to the kinetic restrictions of lithium charge transfer in the SFPE.

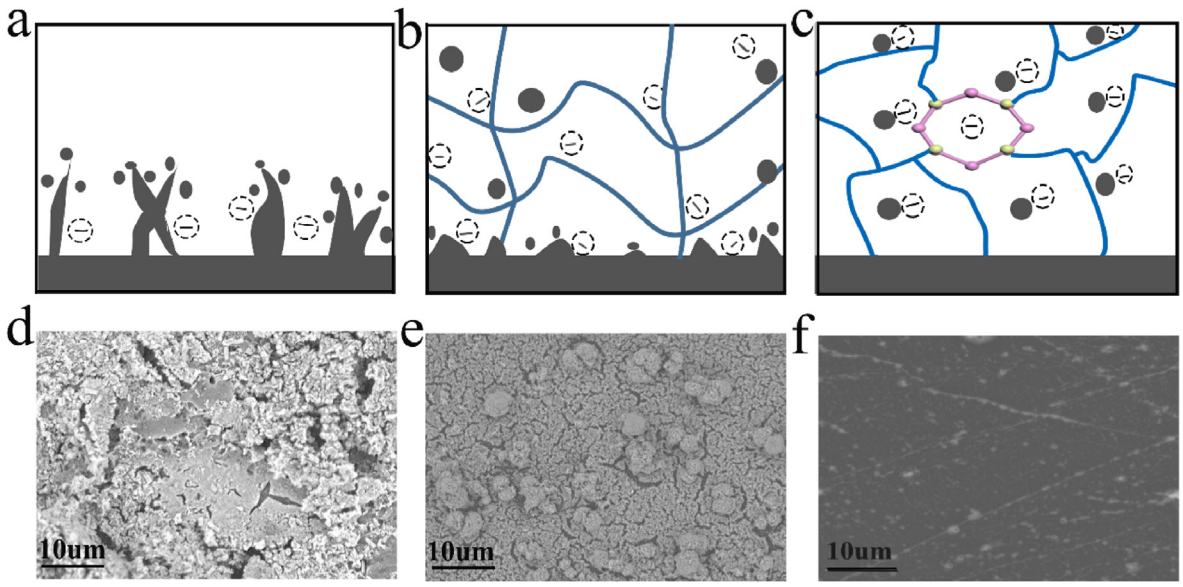

Fig. 4. Illustrations of the electrochemical deposition behavior at the Li anode with (a) a liquid electrolyte, (b) PDDC, and (c) the SFPE (with immobilized anions), and SEM images of the Li metal anode surface in (d) Li/liquid electrolyte/Li (e) Li/PDDC-SPE/Li, and (f) Li/SFPE/Li cells after 600 h of galvanostatic cycling.

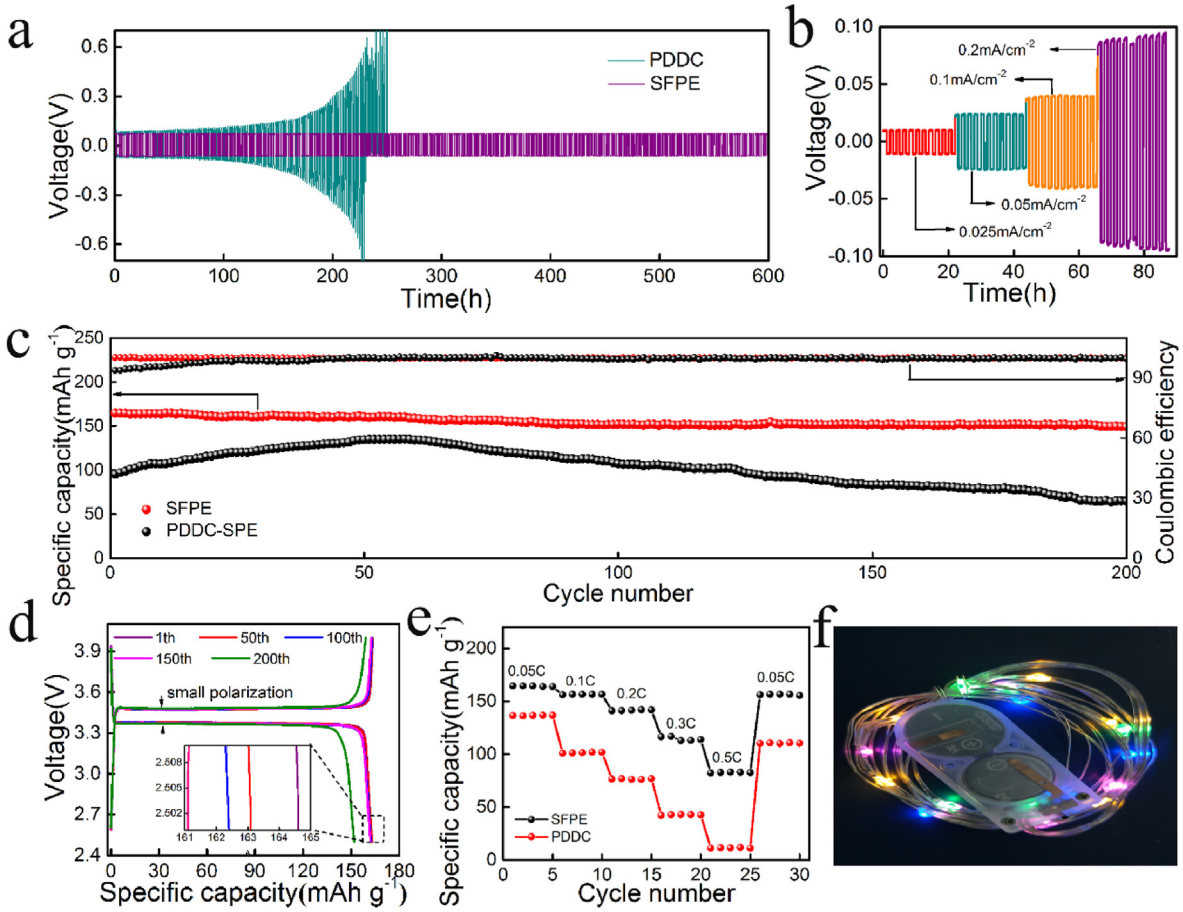

Fig. 5. (a) Voltage profiles of lithium-metal plating/stripping in the Li//Li symmetrical cell cycled under a current density of 0.1 mA cm−2 With SFPE. (b) rate performance of the Li//Li symmetrical cell containing the SFPE under different current densities; (c) cycle performance of the Li/SFPE/Li cell at 0.1 C and 25 °C; (d) typical charge−discharge voltage profiles of the Li/SFPE/Li cell at 0.1 C and 25 °C; (e) rate cycling stability of the cells containing the SFPE and PDDC; (f) practical application of the Li/SFPE/LFP cell.

The cycle performance of the LFP/SFPE/Li cell and that of the LFP/PDDC-SPE/Li cell are shown in Fig. 5c. The specific discharge capacity of the LFP/PDDC-SPE/Li cell increased from 95.2 to 134.9 mAh g^{-1} after 48 cycles, and this discharge capacity was maintained for another 12 cycles. Further cycling, however, led to a continuous decrease in specific discharge capacity, which was only 65.1 mAh g^{-1} after 200 cycles (at which point the capacity retention rate was 48.2%). This behavior occurs because there are defects at the point where the positive electrode was placed in contact with the electrolyte during battery assembly. After initiating the cycling, the polymer segment and lithium ions move, the polymer gradually comes into effective contact with the active particles. After several dozen cycles of activation, the polymer electrolyte forms a stable interface with the positive electrode, but the consumption of anions ($TFSI^-$) at the side of the lithium anode during battery cycling promotes the formation and growth of lithium dendrites due to the resulting space charge. In contrast, the LFP/SFPE/Li cell exhibited excellent cycle performance after 200 cycles, with a specific capacity of 164.6 mAh g^{-1} and capacity retention of 91.3%. This can be attributed to the Si—O—Si structure of VPOSS, which enables the electrolyte to make good contact with the electrode at the start of cycling. Moreover, the addition of VPOSS enables the electrolyte to inhibit the free movement of anions, which suppresses the formation of lithium dendrites. It should also be noted that the coulombic efficiency achieved with PDDC as electrolyte increased from 94.1% after 46 cycles to 99.2% and remained stable, while the coulombic efficiency attained with SFPE as electrolyte remained at 99.2% throughout the cycling period. High Coulomb efficiency proves the excellent electrochemical stability of SFPE and its effective protection on the lithium metal anode.

Typical charge—discharge voltage profiles obtained during the 1st, 50th, 100th, 150th, and 200th cycles at 0.1 C and 25 °C are shown in Fig. 5d. The low polarization observed demonstrates the outstanding interface compatibility and high ionic conductivity of the SFPE. On the other hand, the charge—discharge voltage profiles obtained with PDDC-SPE (depicted in Fig. S8) show high polarization, indicative of poor interfacial compatibility and cycle stability.

As is shown in Fig. 5e, the LFP/SFPE/Li battery exhibited good rate cycling stability and delivered discharge capacities of 165.2, 156.5, 143.0, 112.9, and 81.5 mAh g^{-1} at rates of 0.05, 0.1, 0.2, 0.3, and 0.5 C, respectively. When the rate was returned to 0.05 C, the specific discharge capacity reached 155.8 mAh g^{-1}, which was 94.3% of the initial capacity. In contrast, the discharge capacities of the LFP/PDDC-SPE/Li cell were only 135.7, 101.6, 76.11, 43.33, and 22.96 mAh g^{-1} at 0.05, 0.1, 0.2, 0.3, and 0.5 C, respectively, and the capacity retention rate was only 80.3% when the rate was returned to 0.05 C. Fig. S9 presents typical charge—discharge voltage curves for the LFP/SFPE/Li cell at voltages of 2.0—4.5 V and for rates ranging from 0.1 to 0.5 C at room temperature. The voltage polarization was observed to be very slight and remained almost constant.

The real-world applicability of the assembled LFP/SFPE/Li cell was also tested. Fig. 5f shows that two batteries capable of emitting light from a small bulb. This proves that the SFPE has the potential for practical application in lithium metal batteries.

4. Conclusion

In conclusion, an anion-inhibited solid framework polymer electrolyte (SFPE) was prepared as a means to inhibit the formation of lithium dendrite at the anode of lithium metal battery, which should lead to a safer battery according to space-charge theory. Free movement of anions was effectively inhibited by the use of an electrolyte with an ordered solid framework structure. Further, the lithium-ion transference number of the SFPE was found to be as high as 0.63, and the surface of the lithium metal remained smooth after 600h constant current charge-discharge cycles of Li/SFPE/Li cell. In addition, its high ionic conductivity (0.31 mS cm^{-1}) and wide electrochemical stability window (5.6 V) at 25 °C indicate that the SFPE has the potential to be widely applied in the field of energy storage systems. Finally, the LFP/SPFE/Li cell presented a high specific capacity (165 mAh g^{-1}) and retention rate (91.3% after 200 cycles at 0.1 C) at room temperature. This anion-inhibited solid framework structure polymer electrolyte provides the possibility of the practical application of all solid-state LMBs.

CRediT authorship contribution statement

Wenyan Shang: Conceptualization, Methodology, Investigation, Writing - original draft. **Chaoqun Niu:** Conceptualization, Methodology, Investigation. **Guangping Chen:** Methodology, Validation. **Yubing Chen:** Methodology, Validation. **Jie Du:** Resources, Supervision, Writing - review & editing, Project administration.

Acknowledgements

This work was financially supported by the National Natural Science Foundation of China (Grant No. 21763009), Hainan Provincial Natural Science Foundation of China (Grant No. 519MS020), and the Graduate Students Innovation Research Project of Hainan Province (Hys2019-118, Hys2019-119, Hys2019-120).

Appendix A. Supplementary data

Supplementary data to this article can be found online at https://doi.org/10.1016/j.electacta.2020.135902.

References

[1] S. Zhang, K. Ueno, K. Dokko, M. Watanabe, Recent advances in electrolytes for lithium-sulfur batteries, Adv. Energy Mater. 5 (2015) 28.
[2] D.C. Lin, Y.Y. Liu, Y. Cui, Reviving the lithium metal anode for high-energy batteries, Nat. Nanotechnol. 12 (2017) 194—206.
[3] X.B. Cheng, Q. Zhang, Growth mechanisms and suppression strategies of lithium metal dendrites, Prog. Chem. 30 (2018) 51—72.
[4] C.Q. Niu, J. Liu, G.P. Chen, C. Liu, T. Qian, J.J. Zhang, B.K. Cao, W.Y. Shang, Y.B. Chen, J.L. Han, J. Du, Y. Chen, Anion-regulated solid polymer electrolyte enhances the stable deposition of lithium ion for lithium metal batteries, J. Power Sources 417 (2019) 70—75.
[5] Y. Li, J. Cao, Q. Liu, A.X. Wang, B.H. Li, A sandwich-structure composite membrane as separator with high wettability and thermal properties for advanced lithium-ion batteries, Int. J. Electrochem. Sci. 14 (2019) 7088—7103.
[6] J. Liu, X. Shen, J. Zhou, M. Wang, C. Niu, T. Qian, C. Yan, Non-flammable and high-voltage-tolerated polymer electrolyte achieving high stability and safety in 4.9 V-class lithium metal battery, ACS Appl. Mater. Interfaces 48 (2019) 45048—45056.
[7] H. Duan, Y.X. Yin, Y. Shi, P.F. Wang, X.D. Zhang, C.P. Yang, J.L. Shi, R. Wen, Y.G. Guo, L.J. Wan, Dendrite-free Li-metal battery enabled by a thin asymmetric solid electrolyte with engineered layers, J. Am. Chem. Soc. 140 (2018) 82—85.
[8] J.C. Chai, Z.H. Liu, J. Ma, J. Wang, X.C. Liu, H.S. Liu, J.J. Zhang, G.L. Cui, L.Q. Chen, In situ generation of poly (vinylene carbonate) based solid electrolyte with interfacial stability for LiCoO2 lithium batteries, Adv. Sci. 4 (2017) 9.
[9] F. Lv, Z.Y. Wang, L.Y. Shi, J.F. Zhu, K. Edstrom, J. Mindemark, S. Yuan, Challenges and development of composite solid-state electrolytes for high-performance lithium ion batteries, J. Power Sources 441 (2019) 19.
[10] X.B. Cheng, R. Zhang, C.Z. Zhao, Q. Zhang, Toward safe lithium metal anode in rechargeable batteries: a review, Chem. Rev. 117 (2017) 10403—10473.
[11] M.D. Tikekar, S. Choudhury, Z.Y. Tu, L.A. Archer, Design principles for electrolytes and interfaces for stable lithium-metal batteries, Nat. Energy 1 (2016) 1—7.
[12] Z.Y. Tu, M.J. Zachman, S. Choudhury, S.Y. Wei, L. Ma, Y. Yang, L.F. Kourkoutis, L.A. Archer, Nanoporous hybrid electrolytes for high-energy batteries based on reactive metal anodes, Adv. Energy Mater. 7 (2017) 9.
[13] J.F. Zhang, X.F. Li, Y. Li, H.Q. Wang, C. Ma, Y.Z. Wang, S.L. Hu, W.F. Wei, Cross-linked nanohybrid polymer electrolytes with POSS cross-linker for solid-state lithium ion batteries, Front. Chem. 6 (2018) 10.
[14] Y. Huang, S.-D. Gong, R. Huang, H.-J. Cao, Y.-H. Lin, M. Yang, X. Li, Polyhedral oligomeric silsesquioxane containing gel polymer electrolyte based on a PMMA matrix, RSC Adv. 5 (2015) 45908—45918.
[15] A.G. Kannan, N.R. Choudhury, N. Dutta, Fluoro-silsesquioxane-urethane

hybrid for thin film applications, ACS Appl. Mater. Interfaces 1 (2009) 336–347.
[16] X.Q. Zhang, X.B. Cheng, Q. Zhang, Advances in interfaces between Li metal anode and electrolyte, Adv. Mater. Interfaces 5 (2018) 19.
[17] G.Y. Liu, W. Lu, A model of concurrent lithium dendrite growth, SEI growth, SEI penetration and regrowth, J. Electrochem. Soc. 164 (2017) A1826–A1833.
[18] D.C. Lin, W. Liu, Y.Y. Liu, H.R. Lee, P.C. Hsu, K. Liu, Y. Cui, High ionic conductivity of composite solid polymer electrolyte via in situ synthesis of monodispersed SiO2 nanospheres in poly(ethylene oxide), Nano Lett. 16 (2016) 459–465.
[19] I.M. Shilov, I.V. Verem'ev, Prospectives of the use of infrared spectroscopy in pharmaceutical analysis, Farmatsiia 20 (1971) 76–82.
[20] T. Okumura, S. Nishimura, Lithium ion conductive properties of aliphatic polycarbonate, Solid State Ionics 267 (2014) 68–73.
[21] C.Z. Zhao, X.Q. Zhang, X.B. Cheng, R. Zhang, R. Xu, P.Y. Chen, H.J. Peng, J.Q. Huang, Q. Zhang, An anion-immobilized composite electrolyte for dendrite-free lithium metal anodes, Proc. Natl. Acad. Sci. U. S. A 114 (2017) 11069–11074.
[22] K.L. Xu, Y. Qin, T. Xu, X.H. Xie, J.X. Deng, J.L. Qi, C. Huang, Combining polymeric membranes with inorganic woven fabric: towards the continuous and affordable fabrication of a multifunctional separator for lithium-ion battery, J. Membr. Sci. 592 (2019) 9.
[23] J.J. Zhang, J.F. Yang, T.T. Dong, M. Zhang, J.C. Chai, S.M. Dong, T.Y. Wu, X.H. Zhou, G.L. Cui, Aliphatic polycarbonate-based solid-state polymer electrolytes for advanced lithium batteries: advances and perspective, Small 14 (2018) 16.
[24] F. Han, A.S. Westover, J. Yue, X. Fan, F. Wang, M. Chi, D.N. Leonard, N. Dudney, H. Wang, C. Wang, High electronic conductivity as the origin of lithium dendrite formation within solid electrolytes, Nat. Energy 4 (2019) 187–196.